PNAS

Supporting Information for Immunoglobulin G subclasses confer protection against *S. aureus* bloodstream infection through distinct mechanisms in mouse models

Xinhai Chen[1,2], Haley Gula[1$], Tonu Pius[1$], Chong Ou[3], Margaryta Gomozkova[3], Lai-Xi Wang[3], Olaf Schneewind[†], Dominique Missiakas[1*]

*Corresponding author: Dominique Missiakas

Email: dmissiak@bsd.uchicago.edu

This PDF file includes:

Figures S1 to S6
Tables S1 to S4
Legends for Datasets S1 and S2
SI References

Other supporting materials for this manuscript include the following:

Datasets S1 and S2

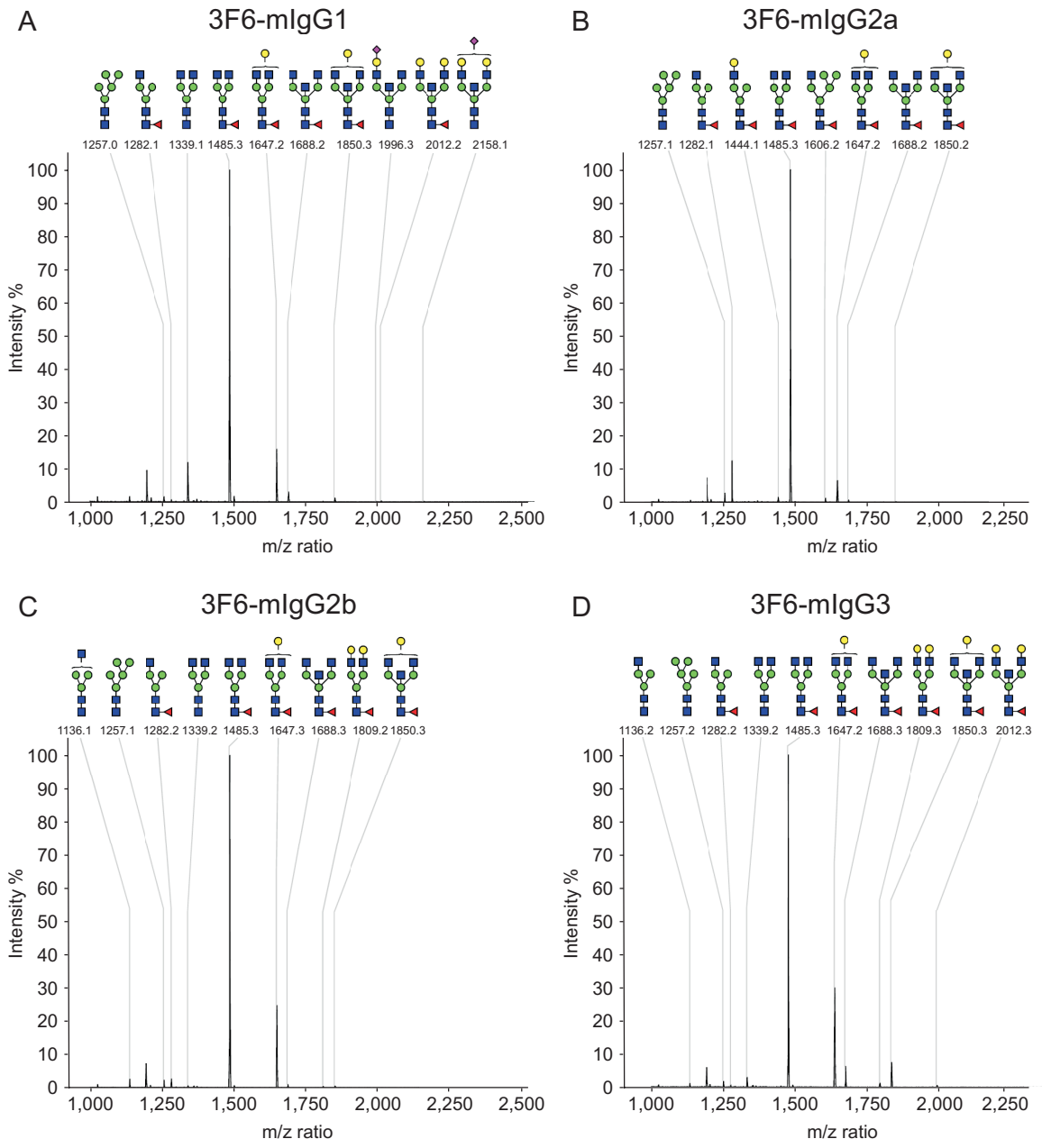

Fig. S1. Analysis of N-glycan composition of 3F6-mIgGs. The N-glycans from the mouse IgG subclasses were released and analyzed as previously described (1, 2). Briefly, the *N*-glycans were released from the respective antibody (100 μg) by treatment with PFNase F (200 units, New England Biolabs) at 37°C in a phosphate buffer (50 mM, pH 7.5, final volume, 50 ml). Released *N*-glycans were isolated with porous graphite carbon solid phase extraction and their composition analyzed by MALDI-TOF MS using a Bruker Autoflex III MALDI-TOF mass spectrometer (Bruker Daltonics) with 2,5-dihydroxybenzoic acid (10 mg/ml in 10% ethanol containing 10 mM NaCl) as the matrix in reflector positive mode.

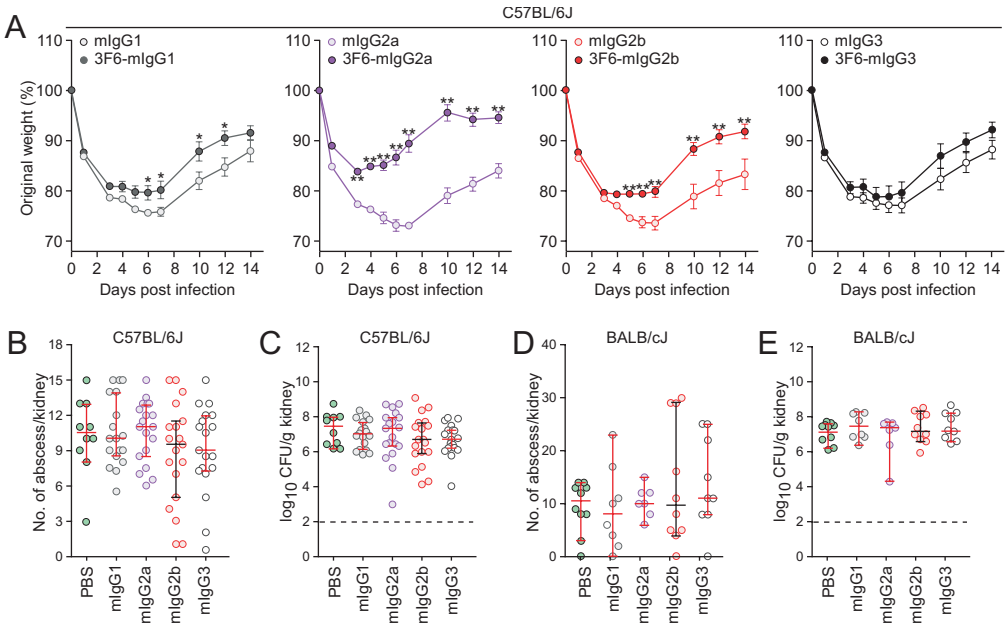

Fig. S2. Impact of passive immunization in mice challenged with *S. aureus* MW2. (A) Body weight of infected mice (n = 10, representative of two independent experiment) shown in panels E, F of Fig. 1 and panels B, C of this figure display. Data were analyzed with the two-way Repeated Measure ANOVA with Bonferroni's multiple comparisons test (*P < 0.05; **P < 0.01). (B-E) Enumeration of tissue surface abscesses (B, D) and bacterial loads in kidney tissues (CFU/g) (C, E) following 15 days infection with *S. aureus* MW2 of C57BL/6J (D, C) or BALB/cJ (D, E) mice. Animals received PBS or 10 mg/kg (body weight, b.w.) subclass control antibodies prior to challenge with *S. aureus*. These experiments were performed in parallel of passive immunization studies shown in Fig. 1E-H. Data are presented as mean ± SEM (A) or medians ± 95% CI (B-E). The dashed line (in C and E) indicates the limit of detection. The complete dataset is analyzed in *SI Appendix*, Table S3.

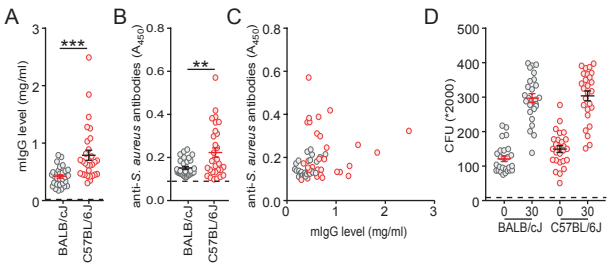

Fig. S3. Pre-existing anti-*S. aureus* antibodies do not have OPK activity. (A) Total mouse IgG titers in sera of naïve BALB/cJ and C57BL/6J mice. (B) Anti-*S. aureus* (anti-SA) titers in sera of naïve BALB/cJ and C57BL/6J mice shown in panel A were measured by ELISA. Live bacteria lacking the immunoglobulin binders SpA and Sbi (Δ*spa*Δ*sbi* bacteria) were coated on the plate and incubated with naïve mouse sera diluted 1:100 in PBS. As a negative control, we use sera from naïve μMT mice that do not produce IgG. This is depicted by the dashed line as the limit of detection. (C) Plot of total versus anti-SA IgG concentrations shown in panels A and B. In general, naïve C57BL/6J mice have higher pre-existing anti-SA antibodies than naïve BALB/cJ mice. However, naïve C57BL/6J mice also produce more total IgGs than naïve BALB/cJ mice. (D) Bacterial survival in blood. CFU of MW2 bacteria incubated for 0 and 30 minutes in freshly drawn, anti-coagulated, mouse blood shown in panel A. A correlation between pre-existing anti-SA antibodies and OPK activity was not observed. Each circle or square represents blood or serum from one animal. Data are presented as mean ± SEM and significant differences were identified with the two-tailed Student's *t* test (***P* < 0.01; ****P* < 0.001).

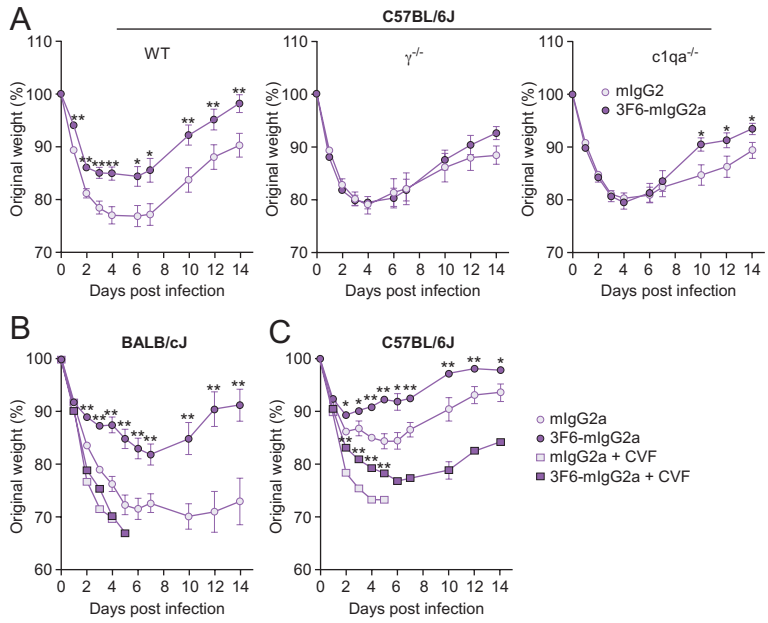

Fig. S4. Body weight of *S. aureus* MW2-infected mice. (A) Body weight of animals shown in Fig. 3A, B and corresponding to C57BL/6J wild-type (WT), γ-/-, and c1qa-/- mice (n = 10, representative of two independent experiment) that received mIgG2a or 3F6-mIgG2a before challenge with *S. aureus* MW2. (B, C) Body weight of animals shown in Fig. 3C and Fig. 3D, respectively. In these experiments, animals received mIgG2a or 3F6-mIgG2a without or with CVF prior to challenge with *S. aureus* MW2. Data are presented as mean ± SEM and analyzed with the two-way Repeated Measure ANOVA with Bonferroni's multiple comparisons test (*P < 0.05; **P < 0.01).

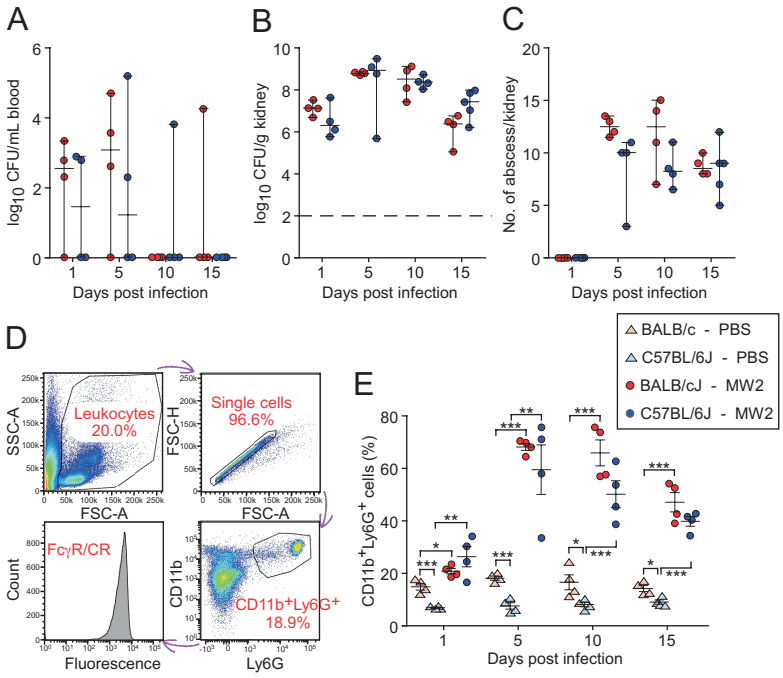

Fig. S5. Surface display of FcγRs and CRs in BALB/cJ and C57BL/6J mice with or without *S. aureus* infection. (A-C) Animals (n = 4 to 5 mice per group) received PBS or *S. aureus* MW2 infection and were euthanized at day 1, 5, 10, or 15 post infection to collect blood and kidneys. Bacterial replication was examined as CFU/ml of blood (A), CFU/g of kidney (B), and surface abscess lesions in kidneys (C). The dashed line in (B) indicates the limit of detection. (D) Flow cytometry scheme for the quantification of $CD11b^{+}Ly6G^{+}$ cells (neutrophils) and quantification of surface levels of FcγRs and CRs shown in Fig. 5. (E) Quantification of neutrophils from the blood of BALB/cJ and C57BL/6J mice infected with PBS or *S. aureus* MW2. Data are presented as medians ± 95% CI (A-C) or mean ± SEM (E). Significant differences were identified with the two-way ANOVA with Tukey test (***P < 0.001; **P < 0.01; *P < 0.05).

.

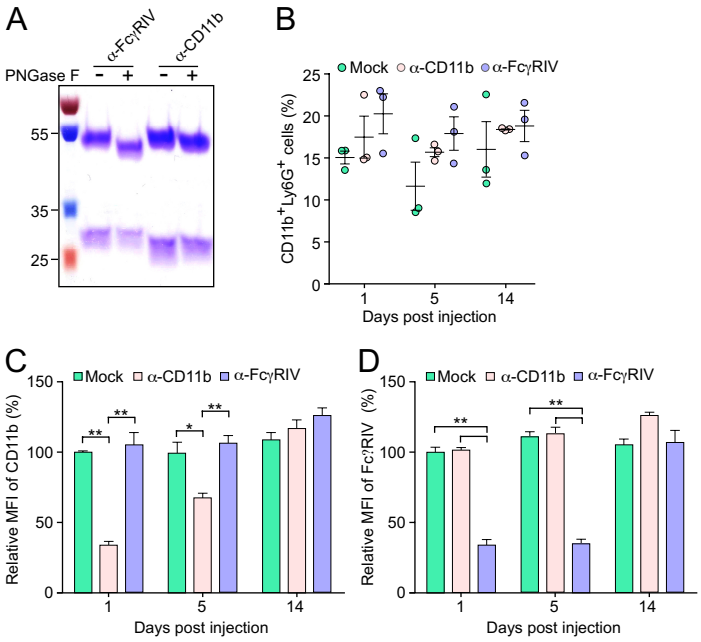

Fig. S6. Employing antibodies to block FcγRIV and CR3 in animals. (A) Coomassie-stained gel of anti-FcγRIV (α-FcγRIV) and anti-CR3 (α-CD11b) following PNGase F treatment. (D) Enumeration of neutrophil on days 1, 5, 14, following injection with mock or PNGase F-treated α-FcγRIV and α-CD11b antibodies in BALB/cJ mice (n = 3). (C, D) Flow cytometry analysis of surface levels of CR3 (C) and FcγRIV (D) on neutrophils from animals shown in panel B. 100% corresponds to the MFI measured for each receptor in the mock (PBS) samples at day one. Data are presented as mean ± SEM. Significant differences were identified with the two-way ANOVA with Tukey test (**P < 0.01; *P < 0.05).

Table S1. Amino acid sequences of the heavy and light chains of 3F6-mIgG antibodies used in this study.

Heavy Chains	
Antibody name and accession number	Amino acid sequence (red variable segment; black constant region)
>3F6-mIgG1 mIgG1: Uniprot No. P01868	MDLRLTYVFIVAILKGVLCEVQLVETGGGLVQPKGSLKLSCAASGFTFNTN AMNWVRQAPGKGLEWVARIRSKSNNYATYYADSVKDRFSISRDDSQNM LSLQMNNLKTEDTAIYYCVTEHYDYDYYVMDYWGQGTSVTVSSAKTTPP SVYPLAPGSAAQTNSMVTLGCLVKGYFPEPVTVTWNSGSLSSGVHTFPA VLQSDLYTLSSSVTVPSSPRPSETVTCNVAHPASSTKVDKKIVPRDCGCK PCICTVPEVSSVFIFPPKPKDVLTITLTPKVTCVVVDISKDDPEVQFSWFVD DVEVHTAQTQPREEQFNSTFRSVSELPIMHQDWLNGKEFKCRVNSAAF PAPIEKTISKTKGRPKAPQVYTIPPPKEQMAKDKVSLTCMITDFFPEDITVE WQWNGQPAENYKNTQPIMNTNGSYFVYSKLNVQKSNWEAGNTFTCSV LHEGLHNHHTEKSLSHSPGK
>3F6-mIgG2a mIgG2a: Uniprot No. P01863	MDLRLTYVFIVAILKGVLCEVQLVETGGGLVQPKGSLKLSCAASGFTFNTN AMNWVRQAPGKGLEWVARIRSKSNNYATYYADSVKDRFSISRDDSQNM LSLQMNNLKTEDTAIYYCVTEHYDYDYYVMDYWGQGTSVTVSSAKTTAP SVYPLAPVCGDTTGSSVTLGCLVKGYFPEPVTLTWNSGSLSSGVHTFPA VLQSDLYTLSSSVTVTSSTWPSQSITCNVAHPASSTKVDKKIEPRGPTIKP CPPCKCPAPNLLGGPSVFIFPPKIKDVLMISLSPIVTCVVVDVSEDDPDVQI SWFVNNVEVHTAQTQTHREDYNSTLRVVSALPIQHQDWMSGKEFKCKV NNKDLPAPIERTISKPKGSVRAPQVYVLPPPEEEMTKKQVTLTCMVTDFM PEDIYVEWTNNGKTELNYKNTEPVLDSDGSYFMYSKLRVEKKNWVERN SYSCSVVHEGLHNHHTTKSFSRTPGK
>3F6-mIgG2b mIgG2b: Uniprot No. A0A075B5P3	MDLRLTYVFIVAILKGVLCEVQLVETGGGLVQPKGSLKLSCAASGFTFNTN AMNWVRQAPGKGLEWVARIRSKSNNYATYYADSVKDRFSISRDDSQNM LSLQMNNLKTEDTAIYYCVTEHYDYDYYVMDYWGQGTSVTVSSAKTTPP SVYPLAPGCGDTTGSSVTLGCLVKGYFPESVTVTWNSGSLSSSVHTFPA LLQSGLYTMSSSVTVPSSTWPSQTVTCSVAHPASSTTVDKKLEPSGPIST INPCPPCKECHKCPAPNLEGGPSVFIFPPNIKDVLMISLTPKVTCVVVDVS EDDPDVRISWFVNNVEVHTAQTQTHREDYNSTIRVVSALPIQHQDWMSG KEFKCKVNNKDLPSPIERTISKIKGLVRAPQVYILPPPAEQLSRKDVSLTCL VVGFNPGDISVEWTSNGHTEENYKDTAPVLDSDGSYFIYSKLDIKTSKWE KTDSFSCNVRHEGLKNYYLKKTISRSPGK
>3F6-mIgG3 mIgG3: Uniprot No. P03987-2	MDLRLTYVFIVAILKGVLCEVQLVETGGGLVQPKGSLKLSCAASGFTFNTN AMNWVRQAPGKGLEWVARIRSKSNNYATYYADSVKDRFSISRDDSQNM LSLQMNNLKTEDTAIYYCVTEHYDYDYYVMDYWGQGTSVTVSSTTTAPS VYPLVPGCSDTSGSSVTLGCLVKGYFPEPVTVKWNYGALSSGVRTVSSV LQSGFYSLSSLVTVPSSTWPSQTVICNVAHPASKTELIKRIEPRIPKPSTPP GSSCPPGNILGGPSVFIFPPKPKDALMISLTPKVTCVVVDVSEDDPDVHV SWFVDNKEVHTAWTQPREAQYNSTFRVVSALPIQHQDWMRGKEFKCK VNNKALPAPIERTISKPKGRAQTPQVYTIPPPREQMSKKKVSLTCLVTNFF SEAISVEWERNGELEQDYKNTPPILDSDGTYFLYSKLTVDTDSWLQGEIF TCSVVHEALHNHHTQKNLSRSPGK
Shared κ light chain	
>3F6	METDTLLLWVLLLWVPGSTGDIVLTQSPASLAVSLGQRATISCRASESVEY SGASLMQWYQHKPGQPPKLLIYAASNVESGVPARFSGSGSGTDFSLNIH PVEEDDIAMYFCQQSRKVPSTFGGGTKLEIKRADAAPTVSIFPPSSEQLT SGGASVVCFLNNFYPKDINVKWKIDGSERQNGVLNSWTDQDSKDSTYS MSSTLTLTKDEYERHNSYTCEATHKTSTSPIVKSFNRNEC

Table S2. Raw data plotted in Fig. 1D to assess the association of SpA to human IgG in the presence of recombinant and hybridoma 3F6 antibodies as well as isotype controls.

	OD_{450} values			Relative hIgG binding		
Experiment #	1	2	3	1	2	3
PBS	3.5441	3.5164	3.5264	100.4288	99.6439	99.92727
mIgG1	3.4486	3.3931	3.3429	97.72266	96.14996	94.72745
3F6-mIgG1	0.4488	0.4438	0.4532	12.7176	12.57592	12.84229
mIgG2a	2.2591	2.2133	2.1778	64.0159	62.71807	61.71211
3F6-mIgG2a	0.1792	0.192	0.2153	5.077973	5.440686	6.100936
hybridoma mAb 3F6	0.7056	0.7052	0.6869	19.99452	19.98319	19.46462
mIgG2b	3.4216	3.411	3.4084	96.95756	96.65719	96.58351
3F6-mIgG2b	0.3532	0.1983	0.2522	10.00859	5.619209	7.146566
mIgG3	2.7463	2.756	2.6511	77.82165	78.09651	75.12397
3F6-mIgG3	0.3322	0.315	0.3198	9.41352	8.926125	9.062142

Table S3. Passive immunization of mice with various 3F6-mIgG antibodies following bloodstream challenge with MW2 (from data shown in Fig. 1E-H; *SI Appendix*, Fig. S2B-E).

Species	**C57BL/7J**					
Data		**Staphylococcal load in renal tissues**			**Abscesses in renal tissues**	
Treatment	**No. of mice[a]**	**$Log_{10}CFU\ g^{-1}$[b]**	***P* value[c]**	**Reduction[d]**	**No. of abscesses/kidney[e]**	***P* value[f]**
PBS	10	7.44 ± (6.62-7.95)			10.50 ± (7.94-12.66)	
mIgG1	18	6.97 ± (6.59-7.39)	0.7069	0.3	10.00 ± (9.08-12.03)	0.9566
3F6-mIgG1	20	5.81 ± (5.47-6.73)	0.0381	1.19	6.38 ± (5.38-8.27)	0.0708
mIgG2a	19	7.34 ± (6.28-7.65)	0.7069	0.33	11.00 ± (9.41-11.91)	0.9566
3F6-mIgG2a	20	6.02 ± (5.31-6.35)	0.0042	1.51	4.75 ± (3.61-6.91)	0.0019
mIgG2b	19	6.70 ± (5.97-7.31)	0.449	0.65	9.5 ± (6.65-10.83)	0.6825
3F6-mIgG2b	20	5.70 ± (5.45-6.03)	0.0035	1.55	8.25 ± (6.94-9.96)	0.6121
mIgG3	19	6.70 ± (6.23-7.12)	0.449	0.61	9.00 ± (7.24-10.84)	0.7287
3F6-mIgG3	20	6.12 ± 1(5.56-6.63)	0.0593	1.1	9.38 ± (6.36-10.09)	0.5469
Species	**BALB/cJ**					
Data		**Staphylococcal load in renal tissues**			**Abscesses in renal tissues**	
Treatment	**No. of mice[a]**	**$Log_{10}CFU\ g^{-1}$[b]**	***P* value[c]**	**Reduction[d]**	**No. of abscesses/kidney[e]**	***P* value[f]**
PBS	20	6.84 ± (6.67-7.19)			9.00 ± (7.18-10.82)	
mIgG1	8	7.40 ± (6.81-8.08)	0.7223	-0.52	8.00 ± (2.58-15.67)	0.9583
3F6-mIgG1	20	5.10 ± (4.17-5.55)	< 0.0001	2.07	6.00 ± (3.66-7.84)	0.2063
mIgG2a	7	7.37 ± (5.76-8.04)	0.9565	0.03	3 ± (-0.49-11.63)	0.3173
3F6-mIgG2a	20	477 ± (3.81-5.13)	< 0.0001	2.46	1.50 ± (1.34-3.76)	0.004
mIgG2b	10	7.20 ± (6.76-7.99)	0.7223	-0.44	9.50 ± (5.40-22)	0.1622
3F6-mIgG2b	20	4.72 ± (4.12-5.29)	< 0.0001	2.23	2.00 ± (1.88-5.62)	0.0296
mIgG3	9	7.22 ± (6.86-8.09)	0.7223	-0.55	11.00 ± (7.27-20.51)	0.1622
3F6-mIgG3	20	5.18 ± (3.63-5.21)	< 0.0001	2.51	3.00 ± (2.25-6.95)	0.0932

[a] Number of 6-week-old female C57BL/6J and BALB/cJ mice.
[b] Staphylococcal load in homogenized renal tissues 15 days following infection. Values are medians ± (lower and upper 95% CI of mean).
[c] *P* value calculated with One-way ANOVA with Kruskal–Wallis's test.
[d] Reduction in bacterial load, calculated as $\log_{10}$ CFU g^{-1}.
[e] Surface renal abscesses. Values are medians ± (lower and upper 95% CI of mean)
[f] P value calculated with One-way ANOVA with Kruskal–Wallis's test.

Table S4. Half maximal effective concentration (EC_{50}) values for all binding experiments using ELISA.

Ligand	EC_{50} (M)	3F6-mIgG1	3F6-mIgG2a	3F6-mIgG2b	3F6-mIgG3	hybri 3F6 (mIgG2a)
SpA_{KKAA} (from Fig. 1C)	10^{-10}	1.689 ± 0.41	1.967 ± 0.73	2.681 ± 0.13	3.088 ± 0.14	2.328 ± 0.66
C57BL/6J C1q (from Fig. 4A)	10^{-8}	<	1.931 ± 0.33	3.972 ± 0.71	3.108 ± 0.73	2.340 ± 0.27
BALB/cJ C1q (from Fig. 4A)	10^{-8}	<	2.129 ± 0.39	3.511 ± 0.59	3.538 ± 0.76	2.684 ± 0.39
C57BL/6J mFcγRIII (from Fig. 4C)	10^{-8}	4.029 ± 0.25	0.636 ± 0.027	0.295 ± 0.134	<	--
BALB/cJ mFcγRIII (from Fig. 4A)	10^{-8}	1.992 ± 0.10	0.536 ± 0.026	0.231 ± 0.094	<	--
mFcRn pH6.0 (from Fig. 4D)	10^{-8}	5.610 ± 0.62	2.344 ± 0.27	2.062 ± 0.41	2.517 ± 0.36	1.639 ± 0.27

Symbols are as follows: -- binding was not measured; < binding was too low to determine association.

Dataset S1 (separate file). Non-synonymous single nucleotide polymorphisms (nsSNPs) in the *C1qa*, *C1qb*, *C1qc*, and *Fcgr3* genes.

Sequences for the *C1qa*, *C1qb*, *C1qc*, and *Fcgr3* genes were retrieved from the Mouse Genome Database (MGD: http://www.informatics.jax.org) and analyzed to identify non-synonymous single nucleotide polymorphisms (nsSNPs) that result in amino acid differences in coding sequences between C57BL/6J and BALB/cJ animals. The data is shown in an excel file with a different sheet for each gene. nsSNPs considered in this study are highlighted in yellow.

Dataset S2 (separate file). SNPs in introns and other untranslated regions of FcγR and complement genes that could result in differential expression.

Sequences were retrieved from the Mouse Genome Database (http://www.informatics.jax.org) and analyzed to identify single nucleotide polymorphisms (nsSNPs) that could result in differential expression of the genes. The data is shown in an excel file with a different sheet for each gene.

SI References

1. Q. Yang, L. X. Wang, Mammalian alpha-1,6-Fucosyltransferase (FUT8) Is the Sole Enzyme Responsible for the N-Acetylglucosaminyltransferase I-independent Core Fucosylation of High-mannose N-Glycans. *J Biol Chem* **291**, 11064-11071 (2016).
2. B. D. Prater, H. M. Connelly, Q. Qin, S. L. Cockrill, High-throughput immunoglobulin G N-glycan characterization using rapid resolution reverse-phase chromatography tandem mass spectrometry. *Anal Biochem* **385**, 69-79 (2009).